Applied Catalysis B: Environmental 163 (2015) 258–266

Contents lists available at ScienceDirect

Applied Catalysis B: Environmental

journal homepage: www.elsevier.com/locate/apcatb

One-pot tandem processing of glycerol stream to 1,2-propanediol with methanol reforming as hydrogen donor reaction

E.S. Vasiliadou[a], V.-L. Yfanti[a], A.A. Lemonidou[a,b,*]

[a] Department of Chemical Engineering, Aristotle University of Thessaloniki, University Campus, GR-54124 Thessaloniki, Greece
[b] Chemical Process and Energy Resources Institute (CERTH/CPERI), P.O. Box 60361 Thermi, Thessaloniki 57001, Greece

ARTICLE INFO

Article history:
Received 20 May 2014
Received in revised form 25 July 2014
Accepted 2 August 2014
Available online 12 August 2014

Keywords:
Copper catalyst
Platinum catalyst
Glycerol hydrogenolysis
Methanol reforming
1,2-propanediol

ABSTRACT

1,2-propanediol is formed efficiently using bio-glycerol feedstock via hydro-deoxygenation reaction with H_2 formed *in-situ* by a novel reaction cycle. The new catalytic route presented here includes the reformation of methanol, remained unreacted after transesterification, for the production of the active H_2 which is consumed in the tandem reaction of glycerol hydrogenolysis. The overall process proceeds in liquid phase over Pt or Cu based catalysts at 220–250 °C and 3.5 MPa initial N_2 pressure for 1 and 4 h reaction time. The test over Pt/SiO_2 catalyst resulted in 1,2-propanediol yield of 21.4%. The yield to the desired product in the presence of Al_2O_3 supported Pt is further limited due to the high extent of the over-hydrogenolysis reactions to propanols, which are promoted by the catalyst acidity. Cu:Zn:Al catalysts showed promising performance in the combined reaction cycle. The Cu bulk catalyst (with 49 wt% Cu) synthesized by the oxalate gel co-precipitation route exhibits ~35% yield to 1,2-propanediol at the standard reaction conditions. Further increase to 1,2-propanediol yield (up to ~45%) was achieved by tuning the reaction conditions. Experiments with labeled $^{13}CH_3OH$ shed light into the H_2 formation origin and proved that ~70% of the total H_2 is indeed produced from the reformation of methanol.

1. Introduction

Production of value added-chemicals via catalytic conversion of biomass derived and renewable sources has attracted much consideration [1]. Glycerol, one of the top 12 building block chemicals and largely available from the biodiesel production process, can serve as a feedstock for the production of valuable chemical products [2–5]. One of the most attractive routes of upgrading glycerol is the formation of 1,2-propanediol (propylene glycol). Propylene glycol, a major commodity chemical currently produced by hydration of the fossil derived propylene oxide, could alternatively be formed using glycerol as a starting material [6]. Glycerol can be converted to propylene glycol over a metal catalyst and H_2 via hydrogenolysis (or hydrodeoxygenation) reaction [7–17] under H_2 pressures up to 10 MPa [18]. As glycerol hydrogenolysis reaction involves C–O bond cleavage and simultaneous hydrogen addition, most of the previous related studies have been carried out under hydrogen pressure providing H_2 from an external source. In spite of these several research efforts, the need to provide H_2 presents one of the main drawbacks of the new glycerol hydrogenolysis technology. These drawbacks are mainly related with the fact that currently H_2 is mainly formed using fossil feedstocks and on the other hand with its properties like flammability and diffusivity.

The concept *of in-situ* hydrogen formation and consecutive consumption overrides the above mentioned problems [19,20]. Within this concept two different approaches have been explored: the hydrogenolysis of glycerol with H_2 produced *in-situ* via reforming part of glycerol (APR – aqueous phase reforming) and H_2 formed by transfer reactions (CTH – catalytic transfer hydrogenation) using 2-propanol or formic acid as donor molecules. The first study was reported in a communication paper from Prof. Jacobs group in 2008 [19]. Glycerol hydrogenolysis was carried out at APR conditions over a Pt/NaY catalyst for propylene glycol formation in the absence of added hydrogen resulting in a 54.6% propylene glycol yield (64% selectivity at 85.4% glycerol conversion) at 230 °C and 15 h reaction time. The above groups have also patented the process of glycerol conversion to 1,2-propanediol in absence of added H_2 [21]. Some other groups have also investigated the possibility of coupling glycerol APR with hydrogenolysis [20–25]. Recently, Barbelli et al. [25] investigated the promotion of Pt with Sn and tested a series of bimetallic catalysts at 2 h batch tests under both H_2 and

* Corresponding author at: Department of Chemical Engineering, Aristotle University of Thessaloniki, University Campus, GR-54124 Thessaloniki, Greece.
Tel.: +30 2310 996273; fax: +30 2310 996184.
E-mail addresses: alemonidou@cheng.auth.gr, alemonidou@gmail.com (A.A. Lemonidou).

http://dx.doi.org/10.1016/j.apcatb.2014.08.004
0926-3373/

N_2 pressure. The best catalytic results were achieved in the presence of the Pt-Sn (Sn/Pt = 0.2) leading to a glycerol conversion to liquid products equal to 54% with 59% propylene glycol selectivity (31.8% yield) at 200 °C and 0.4 MPa pressure. The authors attribute the positive effect of Sn to the existence of Sn^{n+} "acid Lewis sites" which would facilitate the reactant adsorption and C–O cleavage.

On the other hand, the formation of hydrogen via CTH reactions as alternative of using a part of glycerol itself, have been firstly reported in a communication paper by Musolino et al. [26]. The authors exploited the selective transfer of glycerol to propylene glycol over a Pd/Fe_2O_3 catalyst using 2-propanol or ethanol as H_2 sources. They observed that at 180 °C after 24 h glycerol was fully converted to a mixture of propylene glycol and ethylene glycol (94 and 6% selectivity respectively). The combination of CTH with glycerol hydrogenolysis was also studied by Gandarias et al. [27–29]. In their most recent publication [29] the glycerol hydrogenolysis reaction was examined over a $Ni\text{-}Cu/Al_2O_3$ catalyst using formic acid as a hydrogen donor molecule. A glycerol conversion of 90% along with 82% propylene glycol selectivity (73.8% yield) was obtained by increasing the catalyst weight after 24 h reaction time at 220 °C and 4.5 MPa N_2. A reaction mechanism involving the formation of an alkoxide and proposing competitive adsorption between glycerol and propylene glycol was also proposed.

In spite of the significant progress that have been made as above described, there are still some drawbacks related with both APR and CTH methods. In the case of glycerol APR, even though the glycerol hydrogenolysis reaction is an exothermic one ($\Delta H_{513\,K} = -103$ kJ/mol) [30], the strong endothermic ($\Delta H_{523\,K} = 349$ kJ/mol) character of the APR may render the overall process energetically non efficient. In addition, in most of the reported studies concerning glycerol APR as a hydrogen source, the requirement of noble metal catalysts-Pt and Ru based-is essential as the reaction involves C–C bond scission of glycerol [19–22,25]. On the other hand, when H_2 is formed via CTH reactions and although this process allowed higher yields, the addition of a H_2 donor molecule in the reaction mixture (such as 2-propanol or formic acid) is necessary [26–29].

The catalytic system presented for the first time herein (Scheme 1) is the subject of a patent application [31]. It provides proof of concept for the utilization of the glycerol stream, avoiding separation steps after transesterification (e.g. methanol recovery), to run the hydrogenolysis reaction without external addition of H_2 gas. After the final separation step and the removal of the FFAs and the catalyst, the stream which contains glycerol, methanol and water (bio-glycerol) is used as a feedstock and upgraded according to the new concept. It should be underlined that the present route can be directly applied to heterogeneous catalyzed transesterification units where the crude glycerol stream does not contain impurities (catalyst and soaps). The H_2 needed is *in-situ* formed via methanol reformation in liquid phase over the same catalyst as in hydrogenolysis and under identical conditions. The proposed scheme offers certain advantages in terms of process intensification and energy savings conforming to the need for sustainable green processes. It is conducted in liquid phase eliminating the need of heat of vaporization for the oxygenate feedstocks. In addition, the carbon footprint of the process is further lowered because of the use of a single reactor, where the endothermic aqueous phase methanol reforming (APR) and the exothermic glycerol hydrogenolysis are coupled. But most importantly, the one-pot tandem processing of by-product stream reduces drastically the number of steps necessary for the production of propylene glycol, improving thus the efficiency of the process.

The present work explores the potentiality of 1,2-propanediol production from glycerol using methanol APR as the H_2 donor reaction. Within this context the synthesis, characterization and evaluation of Pt and Cu catalysts in the methanol reforming-glycerol hydrogenolysis reaction cycle under inert atmosphere are investigated. In addition, issues like competitive adsorption of methanol and glycerol on the catalytic surface and quantification of the H_2 formation route using labeled methanol ($^{13}CH_3OH$) are also examined.

2. Experimental

2.1. Catalyst preparation

2.1.1. Pt-based catalysts:

Supported (5 wt% Pt) catalysts were prepared using the wet impregnation method. SiO_2 (Saint-Gobain, Norpro, $S_{BET} = 106\ m^2\ g^{-1}$) and $\gamma\text{-}Al_2O_3$ (Saint-Gobain, Norpro, $S_{BET} = 211\ m^2\ g^{-1}$) were used as the support materials. Pt was loaded on the supports using $H_2PtCl_6{\cdot}6H_2O$ as the metal precursor. After solvent removal under vacuum using a rotary evaporator, drying (110 °C) overnight, the solid is treated in flowing air (450 °C) for 3 h and reduced in flowing mixture of hydrogen/nitrogen (250 °C) for 2 h.

2.1.2. Cu bulk catalysts:

The bulk Cu:Zn:Al catalysts were synthesized using the co-precipitation and the gel-coprecipitation of oxalate precursor methods. The metal precursors used were nitrate salts of each component while the atomic composition of the metals was Cu:Zn:Al = 0.34:0.33:0.33 and 0.59:0.31:0.1. The procedure for the samples synthesized via the conventional carbonate co-precipitation method was as follows: the required quantities of the metal nitrates were dissolved in 150 ml distilled water each, to form transparent aqueous metal nitrate solutions. Another 200 ml of distilled water was stirred continuously on a hot plate magnetic stirrer at a constant temperature at 60 °C and pH 6–7. The metals solution was added in a stepwise manner. Precipitation was achieved via drop wise addition of Na_2CO_3 aqueous solution under continuous stirring and a constant pH of 6–7. After aging for 1 h at room temperature, the precipitate was filtered and washed thoroughly with distilled water for three times. The resulting solid was dried overnight at 120 °C and calcined in synthetic air at 350 °C for 4 h (heating ramp 2 °C/min). For the oxalate gel co-precipitation method an alcoholic solution of 20% excess of oxalic acid was injected rapidly into a mixed alcoholic solution of copper nitrate, zinc nitrate, aluminum nitrate at room temperature and vigorous stirring. The ethanol was separated from the gel-like precipitates at 70 °C using a rotary evaporator. The solid dried at 120 °C overnight and calcined at 150 °C for 1 h, 200 °C for 1 h, 300 °C for 1 h and 360 °C for 4 h with a heating ramp 10 °C/min. All Cu:Zn:Al catalysts were finally reduced at 420 °C for 2 h in flowing mixture of hydrogen/nitrogen. These samples will be referred to as CZA-1-X and CZA-2-Y, where 1 stands for lower loading and 2 for higher loading Cu samples and X or Y: coprec. or oxalate respectively for the synthesis method. For comparison reasons a commercial Cu:Zn:Al-Cu-com. (Alfa-Aesar HiFUELTM R120, Low Temperature Water Gas Shift Copper-based) was also tested.

2.2. Catalyst characterization

Surface areas of the samples were determined by N_2 adsorption at −196 °C, using the multipoint BET analysis method, with an Autosorb-1 Quantachrome flow apparatus. Prior to the measurements, the samples were dehydrated in vacuum at 250 °C overnight.

X-ray diffraction (XRD) patterns were obtained using a Siemens D500 diffractometer, with Cu-Kα radiation.

Inductive coupled plasma-atomic emission spectroscopy (ICP-AES) was used for the determination of the chemical composition

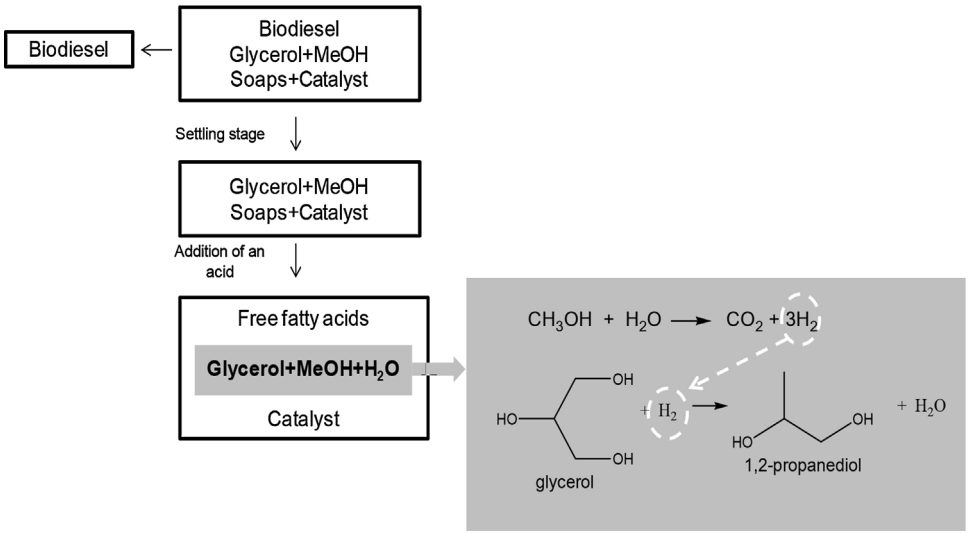

Scheme 1. Proposed process scheme for the one step 1,2-propanediol formation from bio-glycerol stream with *in-situ* H_2 production.

(wt% of Pt) for the fresh catalysts, using a Plasma 400 (Perkin-Elmer) spectrometer, equipped with Cetac6000AT+ ultrasonic nebulizer.

The active copper metal surface area was determined by the dissociative N_2O adsorption method. The experiments performed using the same apparatus as for the TPR. In a typical experiment, the catalyst sample (150 mg) was placed in a U-shaped quartz reactor and pretreated in flowing He (30 cm^3/min) for 0.5 h at 250 °C, followed by cooling at room temperature. The catalyst pre-reduction was performed by raising the temperature to the reduction temperature of every sample with a ramp rate of 10 °C/min in a 10% H_2/He flow (30 cm^3/min) for 0.5 h. Then the sample was exposed to N_2O flow, 30 cm^3/min for 2 h at 50 °C, in order to oxidize the surface Cu^0 to Cu_2O by adsorptive decomposition of N_2O. Finally, TPR was carried out on the freshly oxidized Cu_2O surface in order to reduce the Cu_2O to metallic Cu increasing the temperature from room to 450 °C with 10 °C/min ramp rate using 10% H_2/He flow (30 cm^3/min). Copper surface area and particle size was calculated according to data adopted from literature [32].

2.3. Activity tests

The reaction tests were carried out in a 450 ml stainless-steel batch reactor (Parr Instruments) equipped with an electronic temperature controller and a mechanical stirrer. The reaction was typically conducted under the following standard conditions: 250 °C, 3.5 MPa initial N_2 pressure, 0.1–0.4 weight ratio of catalyst to glycerol, a feedstock mixture of: 7.2 wt% methanol (Panreac 99.5%), 11.4 wt% glycerol (Panreac 99.8%) and water, 4 h reaction time and 1000 rpm stirring rate. The effect of reaction temperature, time and methanol concentration was studied by varying the parameters at ranges of 220–250 °C, 1–4 h and 3.7–11.4 wt% respectively. The reactant conversion and the products electivity and yield were calculated using the equations:

$$\text{Conversion i, \%} = \frac{\text{moles i}_{in} - \text{moles i}_{out}}{\text{moles i}_{in}}$$

where "i" stands for glycerol and methanol. To account for the contribution of methanol formation via the glycerol degradation reaction (glycerol → ethylene glycol + methanol), the term "moles i_{out}" (i = methanol) is corrected by subtracting the equivalent amount of ethylene glycol formed via the above reaction.

$$\text{Selectivity of product i, \%} = \frac{\text{moles C product i}}{\text{C moles of glycerol}_{reacted}} \times 100$$

$$\text{Yield of product i, \%} = \frac{\text{moles of product i}}{\text{moles glycerol}_{in}} \times 100$$

Liquid samples were analyzed by GC (Agilent 7890A, FID, DB-Wax 30 m × 0.53 mm × 1.0 μm). Acetonitrile was used as a solvent for the GC analysis. The multiple point internal standard method was used for the quantification of the results. The liquid products detected were: 1,2-propanediol-1,2-PDO (propylene glycol), ethylene glycol-EG, hydroxyacetone-AC (acetol), 1-propanol-1-PrOH, 2-propanol-2-PrOH and ethanol-EtOH. Low quantities (yielding less than 10%) of side liquid products with 4–6 C atoms were also identified by GC–MS analysis. The GC–MS analysis of the liquid sample revealed that these products were mainly: 1,3-dioxane-5-ol, butane-1,2-diol, butane-2-ol, 1-isopropoxy-propan-2-ol, hexane-2,5-dione. The GC–MS chromatograph is shown in supporting information (Fig. S4). It should be noticed here that these products were only identified in the tests with Cu:Zn:Al catalysts. Gas analysis was performed in an Agilent GC (7890A, Molecular Sieve and Poraplot) equipped with thermal conductivity detector. The gaseous products were mainly CO_2 and H_2. CO, CH_4 and C_2H_6 were also detected at low concentration levels. The total carbon balance in the presence of Pt-catalysts was calculated at range of 82–100%, while over the Cu:Zn:Al catalysts the total carbon balance is between 85 and 90%.

The contribution of methanol reforming to the total H_2 formation was experimentally studied using ^{13}C-labeled methanol (obtained from CORTECNET). For this, a test with glycerol and labeled methanol was conducted and the conversion of $^{13}CH_3OH$ to $^{13}CO_2$ was calculated and compared with the formed $^{12}CO_2$ from glycerol reforming. Based on the stoichiometry of the reforming reactions for both molecules, the ratio of H_2 formed from glycerol and methanol was then calculated. The gas phase products were analyzed using a mass spectrometer (OMNIStar^{TM}, PFEIFFER) following the m/z 44 and 45.

3. Results and discussion

3.1. Catalyst characterization

The composition and the physicochemical properties of the platinum based catalysts are presented in Table 1. The deposition of platinum causes a slight decrease in the specific surface area of the samples compared to the corresponding supports (see Section 2.1). Used catalysts undergo further reduction of the surface area by

Table 1
Physicochemical properties of Pt-based catalysts.

Catalyst	BET surface area ($m^2\ g^{-1}$)		ICP (wt% Pt)		Pt crystallite size (nm)[a]	
	fresh	used	fresh	used	fresh	used
$5Pt/Al_2O_3$	204.2	187.7	5.1	4.6	–	
$5Pt/SiO_2$	92.5	84.1	4.4	4.9	11.7	10.5

[a] Calculated from the XRD patterns.

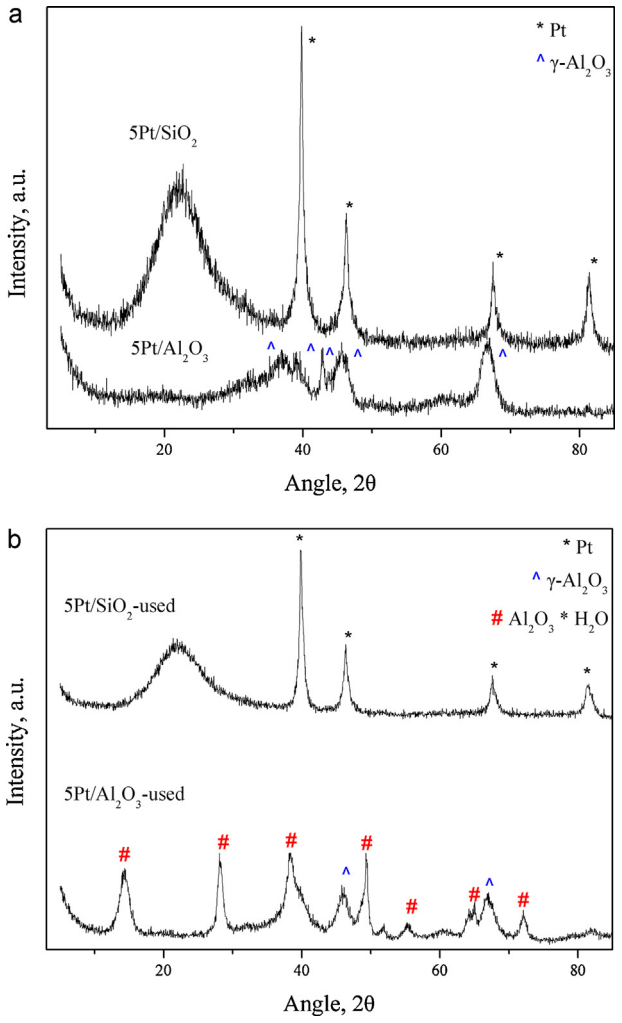

Fig. 1. XRD patterns of Pt-based catalysts: a) fresh reduced and b) used.

10%. The elemental analysis (ICP) data are also shown in Table 1. In both samples, there is a satisfactory agreement between the measured with ICP and the nominal metal composition. Pt loading on the spent catalysts indicates no appreciable metal leaching in the liquid phase after the reaction.

The crystalline phases formed in the fresh reduced and used catalysts were investigated by X-ray diffraction and presented in Fig. 1. The catalyst supported on silica presented a broad peak at about 15–30° due to the amorphous nature of the silica carrier used [33]. The characteristic peak of metallic platinum is only identified on the fresh $5Pt/SiO_2$ catalyst. In the case of fresh reduced $5Pt/Al_2O_3$ only the alumina diffraction peaks were detected probably due to high dispersion of Pt phase. The used catalyst $5Pt/SiO_2$ shows the same pattern with the fresh sample (Fig. 1b). The Pt crystallite size (Table 1) of the fresh and used $5Pt/SiO_2$, as calculated using the Scherrer equation, is similar, pointing out the morphological integrity of the sample. On the other hand, the used

Table 2
Physicochemical properties of Cu bulk catalysts.

Catalyst	Metal composition Cu:Zn:Al (atomic)	BET surface area ($m^2\ g^{-1}$)	S_{Cu} ($m^2\ g_{Cu}^{-1}$)[a]	d_{Cu} fresh (nm)[a]
Cu-com	0.44:0.22:0.34	87.3	83.6	8.1
CZA-1-coprec.	0.34:0.33:0.33	46.2	40.9	16.5
CZA-2-coprec.	0.59:0.31:0.1	38.1	104.8	6.4
CZA-1-oxalate	0.34:0.33:0.33	80.5	144.7	4.7
CZA-2-oxalate	0.59:0.31:0.1	71.5	116.8	5.8

[a] Calculated based on the N_2O surface oxidation data.

$5Pt/Al_2O_3$ undergoes a change as observed by the characteristic lines that correspond to the $Al_2O_3{\cdot}H_2O$ (diaspore) phase (Fig. 1). The latter evidences the unstable structure of alumina under the reaction conditions. This phase transformation has been already reported in literature for Pt/Al_2O_3 catalyst tested in aqueous environment [20].

The metal composition and the porous characteristics of the copper bulk catalysts are presented in Table 2. Compared with the commercial catalyst, Cu-com, all the laboratory synthesized samples show important differences in their porous characteristics. The commercial catalyst presents the largest specific surface area. The oxalate-gel co-precipitation technique leads to the synthesis of materials with BET areas comparable with the commercial catalyst, whereas the conventional co-precipitation results in lower specific areas. Moreover, comparing the samples with different metal compositions it is noticeable that the catalysts with higher Al content – high surface area alumina – (CZA-1-coprec. and CZA-1-oxalate) show higher surface areas, due to the presence of Al_2O_3 [34].

The crystalline phases formed in the fresh copper catalysts were investigated by X-ray diffraction and presented in Fig. 2a. The dominant phase in all samples is CuO. The characteristic diffraction lines of ZnO are broad and especially in the case of the commercial catalyst these peaks are not clearly detected. On the latter sample, the characteristic line (angle 2θ: 26.5°) that corresponds to graphite was also detected. In addition, Al_2O_3 diffraction peaks were not identified in any of the samples. The above observations suggest that these oxides exhibit "X-ray amorphous" features and/or microcrystallites [35]. The different methods used for catalyst synthesis seem to affect the crystalline structure of the materials. From the XRD patterns it is obvious that the samples prepared by the oxalate gel co-precipitation method exhibit broader peaks of both CuO and ZnO phases. This evidences the existence highly dispersed Cu and Zn oxides. It is interesting to notice that for the samples prepared with the conventional co-precipitation method the formation of $NaNO_3$ was also observed. The presence of $NaNO_3$ crystallites is due to the high content of Na owing to the use Na_2CO_3 during the synthesis procedure. ICP analysis of these samples further corroborates the presence of residual sodium. Its concentration was found to be equal to 7.7 wt% and 2.3 wt% for the CZA-1-coprec. and CZA-2-coprec. samples respectively. This observation has been previously reported for a Cu/SiO_2 catalyst prepared by the same method [36]. The authors of the above study also reported a decrease of the BET surface area with increasing the Na content attributed to pore blocking by the $NaNO_3$ crystallites. These observations also explain our data concerning the porous characteristics already presented in Table 2. After the pre-reduction treatment of the conventional co-precipitation synthesized samples (Fig. 2b) it was observed that the peak corresponding to $NaNO_3$ almost disappeared implying that $NaNO_3$ is decomposed and a very small part which still remains is converted to $NaNO_2$. The latter combined with the active Cu areas and the Cu particle sizes (see Table 2) indicate that the initial incorporation of Na leads to irreversible structural changes. Although it is difficult to explain clearly how Na affects the morphology, it has been reported that Na inhibits the interaction between CuO

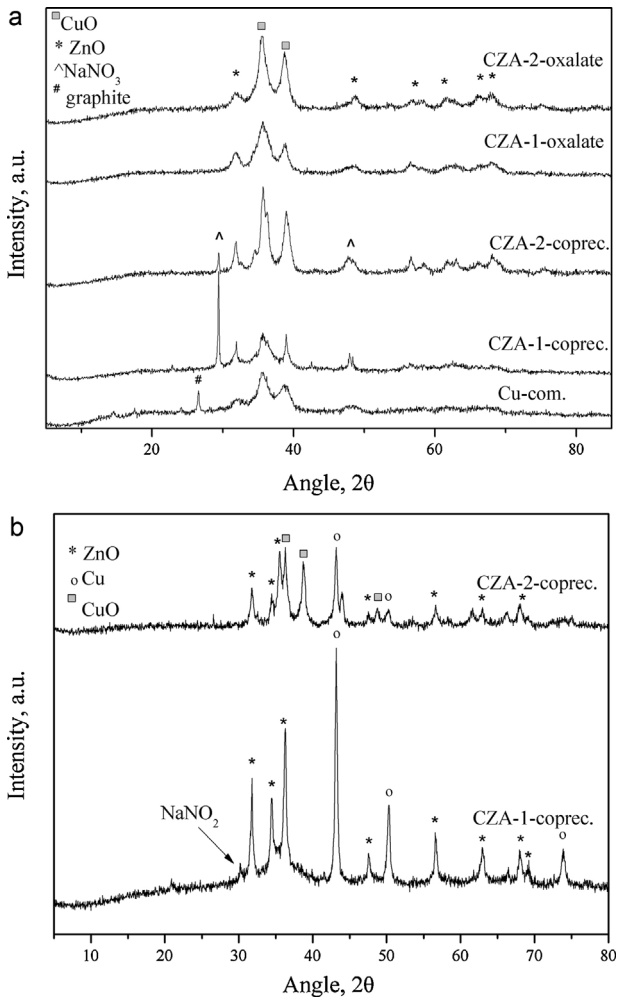

Fig. 2. XRD patterns of: a) fresh calcined and b) reduced samples prepared by the conventional co-precipitation method.

and ZnO increasing the crystallinity of CuO and ZnO and thus the crystallite particle size [37]. After the application of the samples to the reaction conditions and as pre-reduction takes place, the dominant crystalline phase in all samples is metallic copper Cu^0 (see Fig. S3).

The active Cu surface area and the particle size, as measured by the surface oxidation using the N_2O technique are also shown in Table 2. The copper surface area, particle size and consequently the morphology are slightly affected by the different synthesis methods used. In contrast to the other synthesized catalysts, which exhibit satisfactory active Cu areas the CZA-1-coprec. sample presents significantly lower copper surface area. This result was expected due to the existence of the residual Na, which as mentioned above, inhibited the dispersion of copper. The commercial catalyst presents somehow moderate active Cu area, nevertheless higher compared with the CZA-1-coprec. For the oxalate gel synthesized samples and the CZA-2-coprec. catalyst it seems that copper is highly dispersed with the Cu particle size ranging between 4.7 and 6.4 nm.

The reducibility of the catalysts was evaluated with H_2-TPR (supporting information). The profiles of H_2 consumption clearly show that Pt and the Cu based catalysts are fully reduced at temperatures over 250 and 420 °C respectively ensuring that the conditions applied for the prereduction were sufficient.

3.2. Catalyst evaluation

The two series of the synthesized Pt-based and Cu bulk catalysts were tested under reaction conditions to proof the novel concept. It is worthy to underline that these two classes of materials were selected for the combined reaction cycle based on their promising performance in methanol aqueous phase reforming [35,38] and glycerol hydrogenolysis reactions as well [16,39,11]. The catalytic results obtained over the Pt (5 wt%) supported catalysts are summarized in Table 3.

These experimental results clearly demonstrate that 1,2-propanediol is produced under inert conditions (N_2 pressure), with H_2 formed *in-situ* via reforming of the methanol already present in crude glycerol streams. The presence of the Pt supported catalysts results in high glycerol conversion levels from almost 60% to 70% (entries 1 and 2 experiments at 250 °C), while methanol is converted at 25.5–28.0%. The high activity of the Pt-based materials was somewhat expected, as platinum catalysts are known to be effective in both reforming and hydrogenolysis reactions [38,11]. Of interest to see that the rates of glycerol and methanol are in the same range for both materials at the standard reaction conditions, revealing the ability of Pt to catalyze efficiently both reactions. The main output of the latter observation is that over the platinum catalysts tested, the reformation of methanol and the hydrodeoxygenation of glycerol can proceed in a tandem way. The Pt/Al_2O_3 supported catalyst presents slightly higher activity in terms of both glycerol conversion and mass specific rate compared with the SiO_2 based sample, more probably due to its higher acidity that promotes the first step of glycerol dehydration (two step dehydration–hydrogenation mechanism). The latter agrees with our previous results concerning the effect of acidity in both activity and selectivity in glycerol hydrogenolysis reaction [8]. However, the target product yield does not follow this trend. 1,2-propanediol yield is more than three times higher over the silica supported catalyst, due to the poor selectivity obtained in the case of $5Pt/\gamma\text{-}Al_2O_3$ (Table 3). The main reason for the low selectivity over this sample is the excessive sequential hydrogenolysis of the target product to mono-alcohols (propanols). The highest yield to 1,2-propanediol (21.4%) obtained with the present system over Pt-based catalysts is in the same range or even higher than that reported in relevant literature studies in which the required H_2 is formed *in-situ* from glycerol reforming over noble metal catalysts [12,19].

It should be underlined that the intermediate glycerol dehydration product, hydroxyacetone (acetol), was always detected in the product mixture supporting the proposed two-step dehydration–hydrogenation mechanism for glycerol hydrogenolysis [17]. At the standard reaction conditions acetol selectivity is very low, 1.6 and 2.4% for the Pt catalysts tested. Apart from C_3 containing products, others like ethylene glycol (EG), CH_4 and C_2H_6 even though at low selectivities (EG: 1.7–7.2%, CH_4: 0.5–2.7% and C_2H_6: 0.7–5.5%) are formed indicating the ability of Pt for C–C scission reactions. The low reaction temperature favors the water gas shift reaction and thus CO formation is limited to selectivity values up to 0.06%.

The reaction conditions can greatly influence the reaction sequence of methanol reforming-glycerol hydrogenolysis (Table 3, entry 3). A temperature decrease from 250 to 220 °C leads to a decrease in glycerol conversion from about 59 to 20% (over three times lower mass specific rate) as well as in 1,2-PDO yield. The same trend, is observed for methanol conversion and rate as well (from 27.9 to 14.4% and from 13.0 to 7.0 mmol h^{-1} g_{cat}^{-1} respectively). Although glycerol conversion levels are different at 220 and 250 °C and thus a straightforward comparison of the product selectivity is risky, some points are worth mentioning. The selectivity to the desired diol obtained at lower temperature reaches ~66%, a value remarkably higher than that of the selectivity at 250 °C.

Table 3
Catalytic results over Pt supported catalysts under inert atmosphere, standard conditions: 3.5 MPa N_2 initial pressure, 4 h, 250 °C, 7.2 wt% MeOH, 11.4 wt% glycerol (glycerol/methanol molar ratio = 0.55) and water, catalyst/glycerol weight ratio = 0.1.

Catalyst	Conversion (%)		Integral mass specific rate (mmol h^{-1} g_{cat}^{-1})		Carbon selectivity (%)			Yield 1,2-PDO (%)
	Glycerol	Methanol	Glycerol	Methanol	1,2-PDO	Propanols	Acetol	
5Pt/γ-Al_2O_3	70.4	25.5	19.0	13.0	9.5	37.1	1.6	6.7
5Pt/SiO_2	58.9	27.9	16.0	13.0	36.2	25.6	2.4	21.4
5Pt/SiO_2[a]	19.0	14.4	5.0	7.0	65.6	23.9	4.4	12.6
5Pt/SiO_2[b]	43.2	17.1	12.0	4.0	37.9	14.6	23.2	16.4

[a] Reaction Temperature 220 °C.
[b] Methanol concentration 3.7 w/w% (glycerol/methanol molar ratio = 1.1).

At the higher reaction temperature 250 °C, the formation rate of degradation products (ethylene glycol, methane and ethane-not shown) is favored decreasing thus the selectivity to 1,2-PDO. The temperature increment from 220 to 250 °C enhances the glycerol and methanol rates as well as the consumption rate of the target product to C1 and C2 compounds. The increased activity induced by temperature increment towards degradation routes has been also previously reported for noble metal catalysts such as Ru and Rh-based [40,41]. A decrease by half in methanol concentration lowers the conversion and the mass specific rates of both reactants, showing, as expected, a more pronounced effect on methanol rates (Table 3 compare entry 4 and 2). Higher methanol concentration seems to favor 1,2-propanediol yield over the Pt-based catalysts, mainly by enhancing glycerol conversion. An explanation for this could be the tandem way that reforming and hydrogenolysis proceed. Specifically, H_2 formed from methanol is consumed by glycerol contributing thus in high conversion levels and thus higher yields. We have also observed that the selectivity to 1,2-propanediol in both experiments is similar (36.2 and 37.9%), while the selectivity to propanols increase at higher methanol concentration conditions. It is likely that 1,2-propanediol reacts further to propanols due to the higher H_2 availability formed with high rates from methanol. On the other hand, the increased selectivity (23.2%) of the acetol in methanol "poor" feedstocks implies that the hydrogenation rate of the intermediate is insufficient due to the lower hydrogen availability.

Cu catalysts were also tested in this novel catalytic reaction cycle. The ability of Cu-based materials to drive the combined reforming-hydrogenolysis cycle was studied using first a commercial CuO/ZnO/Al_2O_3 (Cu-com) catalyst and thereafter the synthesized Cu bulk catalysts. Table 4 summarizes the experimental results obtained. The commercial catalyst leads to about 70% glycerol conversion, but as the selectivity to 1,2-propanediol is quite low, the yield of the desired product is limited to 16.4%. On the other hand, all the synthesized Cu:Zn:Al catalysts present better performance in terms of activity (glycerol conversion and mass specific rate), 1,2-propanediol selectivity and therefore yield of the desired polyol. Comparing the samples with different Cu loadings prepared by the same method, it is observed that the yield is positively affected by an increase in Cu loading. The effect is more pronounced with Cu catalysts prepared via the oxalate method in which the increase of Cu loading from 25 to 49 wt% results in enhancement of glycerol and methanol conversion and of 1,2-PDO selectivity. In the case of the conventional co-precipitation synthesized samples, the increase of Cu loading does not remarkably affect the catalytic results. This can be attributed to a promoting effect of residual sodium found on the 25 wt% Cu-containing catalyst prepared by this method, thus leading to enhanced catalytic performance of this sample (see also Fig. 4). In general, Cu bulk catalysts seem not to promote the sequential hydrogenolysis to propanols, as well as the C–C cleavage reactions to ethylene glycol (0.6–1.9% selectivity). Worthy also to notice that methane and ethane were not detected in any of the tests using Cu catalysts. The intermediate hydroxyacetone (acetol) was also detected supporting the proposed two-step dehydration–hydrogenation mechanism for hydrogenolysis reaction [17]. The CZA-2-oxalate catalyst containing 49 wt% Cu (atomic 0.59:0.31:0.1) exhibits the highest 1,2-propanediol yield ~35% at the standard reaction conditions, which is further increased to 44.9% upon a decrease of the reaction temperature at 220 °C (Table 4). Lower reaction temperature favors the selectivity of the desired polyol which reaches the value of ~52%. The increase of 1,2-PDO selectivity is mainly associated with the limitation of its sequential hydrodeoxygenation to propanols (Table 4), which is favored under excess hydrogen and higher temperatures [17]. In addition, at lower reaction temperatures the formation of side products (liquid products with C4–C6 as identified using GC–MS), which indirectly affect the 1,2-PDO selectivity, is noticeably decreased. Another interesting point to observe is that over CZA-2-oxalate catalyst, a decrease in the reaction temperature mainly affects the reformation of methanol as its mass specific rate decreases almost four times, while the rate of glycerol conversion decreases only by 37%.

Comparing the performance of the Cu bulk catalysts with the Pt-based in terms of integral mass specific rates (Tables 3 and 4) it is obvious that noble metal catalysts, despite their significantly lower metal loading, exhibit better performance on the overall reaction cycle (both methanol aqueous phase reforming and glycerol hydrodeoxygenation). In the presence of Cu catalysts, the mass specific rates of glycerol conversion prevail over the methanol rates, however in all cases the values are of the same order of magnitude. A possible explanation for this is the competitive adsorption between methanol and glycerol as will be discussed below. Concerning the product distribution over the two series of catalysts tested, interesting observations have been obtained. For both Pt and Cu catalysts, the primary hydrodeoxygenation route results in 1,2-propanediol formation with comparable selectivities (Tables 3 and 4). However, their performance on the sequential hydrodeoxyganation leading to propanols is clearly different. Over the Pt-based catalysts, propanols selectivity is in all cases higher (14.6–37.1%) compared with Cu catalysts (0.4–8.1%) despite the significantly higher conversion levels of the latter. This maybe due to the higher relative mass specific rates between methanol (hydrogen formation) and glycerol (hydrogen consumption) over the Pt (ratio 0.33–1.4) and Cu (ratio 0.12–0.28) catalysts. Further differences in the product distribution are related with the extent of degradation and condensation routes. Degradation (formation of ethylene glycol, methane and ethane), is clearly favored in the presence of Pt metal and not with Cu-based materials. On the contary, Cu-based catalysts promote condensation reactions leading to the formation of C4–C6 liquid products. Nevertheless, the lower ability of Cu on C–C bond cleavage (selective to C_3 products) compared with Pt and its low cost point out the potential of this class of materials on the methanol reforming-glycerol hydrodeoxygenation cycle. Moreover, hydrogen conversion (defined as H_2 consumed for glycerol conversion to products that consume hydrogen/total H_2 formed) in the presence of the Cu:Zn:Al catalysts

Table 4
Catalytic results over Cu bulk catalysts under inert atmosphere, 3.5 MPa N_2 initial pressure, 4 h, 250 °C, 7.2 wt% MeOH, 11.4 wt% glycerol (glycerol/methanol molar ratio = 0.55) and water, catalyst/glycerol weight ratio = 0.4.

Catalyst	Conversion (%)		Integral mass specific rate (mmol h^{-1} g_{cat}^{-1})		Carbon selectivity (%)			Yield 1,2-PDO (%)
	Glycerol	Methanol	Glycerol	Methanol	1,2-PDO	Propanols	Acetol	
Cu-com	70.5	8.1	4.8	1.0	23.3	3.1	5.6	16.4
CZA-1-coprec.	82.7	8.5	7.2	1.3	30.9	1.6	6.6	25.5
CZA-2-coprec.	84.0	10.3	7.3	1.6	34.7	2.8	7.1	29.2
CZA-1-oxalate	76.3	9.9	6.0	1.3	28.4	4.7	6.0	21.7
CZA-2-oxalate	88.8	14.1	6.7	1.9	39.2	8.1	5.4	34.8
CZA-2-oxalate[a]	86.6	5.7	4.2	0.5	51.9	0.1	5.0	44.9

[a] Reaction temperature 220 °C and adjustment of the catalyst weight (catalyst/glycerol weight ratio = 0.6) in order to obtain similar conversion levels.

ranges between 60 and 65%, while for Pt-based catalysts H_2 is significantly lower (35–49%). The latter proves the superiority of Cu catalysts for this cascade system.

Mainly metallic copper, but in some cases Cu^+ or Cu^0–Cu^+ couples are recognized as the active sites for methanol reforming reaction, while Cu^0 has been generally accepted as the active site for glycerol hydrodeoxygenation reaction [15,42–45]. In the latter case, Cu^+ is believed to provide a stabilizing character to Cu catalysts [45]. It has been reported that the activity in methanol reforming as well as in glycerol hydrodeoxygenation is proportional to the active copper surface area [15,16,46]. The activity expressed as moles of reactant consumed per g_{Cu} per hour is plotted vs. Cu active area for the present catalysts (Fig. 3). It can be seen that a clear correlation exists as both methanol and glycerol rates increase almost proportionally with the active copper area (m^2 g_{Cu}^{-1}), implying that metallic copper provides the active sites for the activation of the two reactants. A clear deviation from linearity is observed for the CZA-1-coprec. catalyst, which in spite of the low Cu surface area demonstrates the highest activity. This result is related with the existence of residual Na on this sample, however it is not possible to provide a clear explanation. We can only speculate that this is due to the increased intrinsic activity exhibited by this sample owing to a promotional effect of the residual Na. However, similar observations have been reported previously for glycerol hydrogenolysis over a Cu/SiO_2 catalyst [36].

A study of the effect of the reaction time (0.5–4 h) was performed over the most efficient (in terms of 1,2-PDO yield) CZA-2-oxalate catalyst. The evolution of the products as a function of time is depicted in Fig. 4. The product distribution is quite interesting as the yield of the main product (propylene glycol) presents a maximum value (42.5%) at 1 h. The distribution of the intermediate product (hydroxyacetone) and of the over-hydrogenolysis products (propanols) explains the maximum value obtained. At the initial reaction time of 0.5 h, the H_2 produced from methanol aqueous phase reforming is not sufficient for the hydrogenation of the intermediate hydroxyacetone resulting from glycerol dehydration. With the increase of reaction time the amount of H_2 formed from methanol reformation is enough for the hydrogenation of hydroxyacetone and thus the yield of 1,2-propanediol increases. As the reaction further progresses, the desired product undergoes sequential hydrogenolysis to propanols. Therefore, the optimum reaction time for maximizing the 1,2-propanediol yield seems to be 1 h. This reaction time is much shorter compared with reported studies, in which, times up to 24 h have been applied [12,26,27]. It is very important to stress out that the results of the product distribution with time provide strong evidence about the proposed two-step dehydration–hydrogenation mechanism for hydrogenolysis of glycerol to propylene glycol [17]. Although the yield obtained in the present work is lower compared with previous reports, the productivity ($g_{1,2-PDO}$ g_{cat}^{-1} h^{-1}) of 1,2-propanediol is superior. The maximum productivity of 1,2-propanediol obtained in the present study at 1 h reaction time equals to 1.0 $g_{1,2-PDO}$ g_{cat}^{-1} h^{-1}. Previous reports in which hydrogen is formed via CTH reaction of a hydrogen donor molecule (formic acid and 2-propanol) report productivity values between 0.05 and 0.17 $g_{1,2-PDO}$ g_{cat}^{-1} h^{-1} in the presence of $Ni\text{-}Cu/Al_2O_3$ (at 220 °C) and Pd/Fe_2O_3 (at 180 °C) catalysts [26,29].

3.2.1. Individual reactions of methanol and glycerol

Taking into account the complexity of the present reaction cycle, diagnostic experiments using the individual compounds

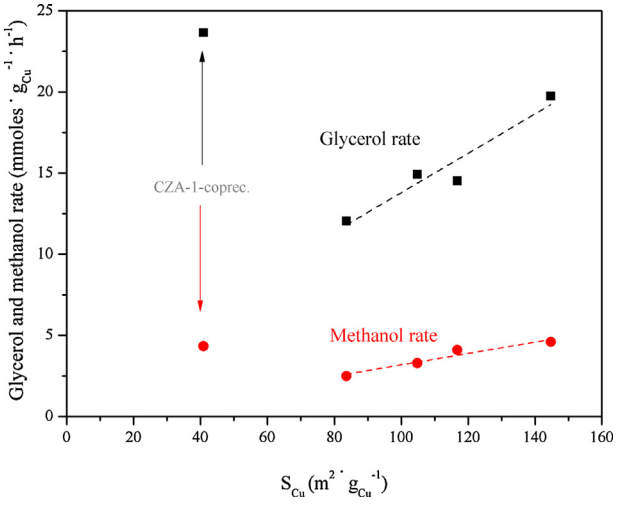

Fig. 3. Correlation between catalytic activity and active copper area for Cu:Zn:Al catalysts, 3.5 MPa N_2 initial pressure, T = 250 °C, 4 h, catalyst/glycerol weight ratio = 0.4, 7.2 wt% MeOH, 11.4 wt% glycerol and water.

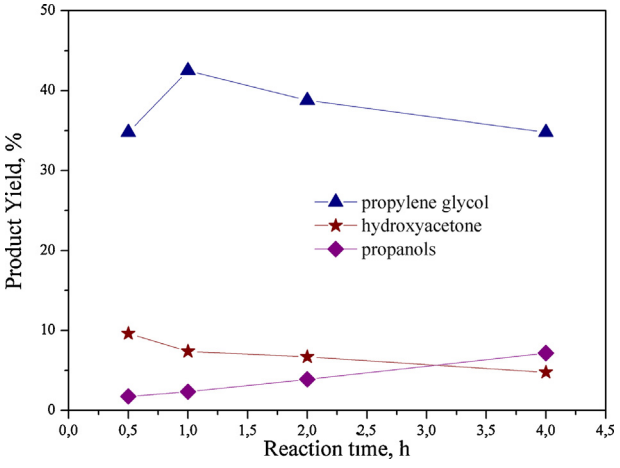

Fig. 4. Effect of reaction time on main product yield over the CZA-2-oxalate catalyst, 3.5 MPa N_2 initial pressure, T = 250 °C, catalyst/glycerol weight ratio = 0.4, 7.2 wt% MeOH, 11.4 wt% glycerol and water.

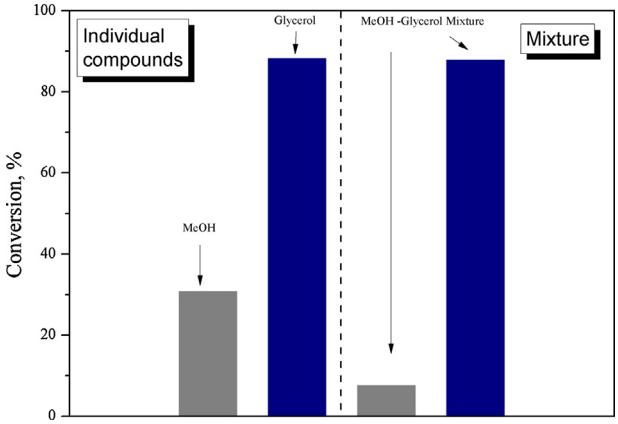

Fig. 5. Conversion of the individual compounds and the combined feedstock over the CZA-2-oxalate catalyst, 3.5 MPa N_2 initial pressure, 1 h, 250 °C, catalyst/glycerol weight ratio = 0.4, methanol reforming: 8 wt% methanol aqueous solution, glycerol reforming: 12 wt% glycerol aqueous solution, combined feedstock: 7.2 wt% MeOH, 11.4 wt% glycerol and water.

methanol and glycerol in mixtures with water as feedstock were also performed. These tests aimed to understand the ability of the CZA-2-oxalate catalyst to reform methanol and to convert glycerol under inert atmosphere. Fig. 5 presents the conversion of the individual compounds and of the combined feedstock. The conversion of methanol as regards to the methanol reforming reaction (water–methanol feedstock) reaches the value of 31%. The main reactions taking place are:

$$CH_3OH + H_2O \rightarrow 3H_2 + CO_2 \quad \Delta H = 49.7\,kJ\,mol^{-1} \tag{1}$$

$$CO + H_2O \leftrightarrow CO_2 + H_2 \quad \Delta H = -41.2\,kJ\,mol^{-1} \tag{2}$$

$$CH_3OH \rightarrow 2H_2 + CO \quad \Delta H = 90.2\,kJ\,mol^{-1} \tag{3}$$

It has been reported that methanol decomposition reaction (3) proceeds along with the steam reforming reaction (1), especially at low methanol conversions [47]. In the methanol aqueous phase reforming experiment, the main products detected were H_2 and CO_2. Both the high activity of the CZA-2-oxalate catalyst towards the water gas shift reaction (2) and the low reaction temperature (250 °C) results in very low CO selectivity in the gas phase equal to 0.2% (not shown). Methane was also formed via the methanation reaction though at very low selectivity of 0.1% (not shown).

The activity of the CZA-2-oxalate catalyst towards glycerol conversion (water–glycerol feedstock) under inert atmosphere is also presented in Fig. 5 (second bar). Compared with methanol APR, glycerol presents higher conversion (88%). The reaction scheme under the present conditions includes the glycerol aqueous phase reforming route (reaction (4)) and the hydrogenolysis route with 1,2-propanediol being the main liquid product formed.

$$C_3H_8O_3 + 3H_2O \leftrightarrow 7H_2 + 3CO_2 \quad \Delta H = 128\,kJ\,mol^{-1} \tag{4}$$

$$C_3H_8O_3 + H_2 \rightarrow C_3H_8O_2 + H_2O \quad \Delta H = -103\,kJ\,mol^{-1} \tag{5}$$

When water–glycerol mixture is used as a feedstock under nitrogen atmosphere the reaction cycle includes the reformation of a part of glycerol (reaction (4)) leading to the production of H_2 and CO_2. The remaining glycerol hydrodeoxygenates using the above produced H_2 forming 1,2-propanediol (selectivity = 30.4%) and hydroxyacetone (selectivity = 9.8%). The conversion of the combined feedstock (water–methanol–glycerol) is also depicted in Fig. 5. The presence of both reactants affects in different way their conversion. The conversion of glycerol seems be independent of methanol presence, while that of methanol drops drastically (from 31% to 8%). The fact that glycerol conversion is similar in both cases, implies the competive adsorption between the two reactants with glycerol strongly adsorbed on the catalytic active surface. On the other hand, the decrease of methanol conversion proves that methanol and glycerol compete for the same Cu active sites. Indeed, the calculation (using VASP – PW91, 3 × 3 cells, 5 × 5 × 1 k-points, PAW pseudopotentials [48]) of the binding energies for the two oxygenated species on Cu(1 1 1) (methanol = −0.28 eV and glycerol = −0.49 eV) supports the above hypothesis. Most importantly, the yield of the desired product is 42.5%, almost 40% higher compared with the case in which glycerol is the source of H_2 (yield = 26.9%). This result suggests that methanol reforming is essential for the high 1,2-propanediol yield.

Table 5
Experiments using labeled $^{13}CH_3OH$ (3.5 MPa N_2 initial pressure, 1 h, 250 °C).

Experiment	Feedstock	Mass specific rate (mmol h^{-1} g_{cat}^{-1})		Ratio *m/z* 44/45
		Glycerol	Methanol	
1	8 wt% $^{12}CH_3OH$ aqueous solution	–	13.0	50.2
2	8 wt% $^{13}CH_3OH$ aqueous solution	–	12.9	0.06
3	7.2 wt% $^{12}CH_3OH$ + 11.4 wt% glycerol aqueous solution	23.4	2.0	51.0
4	7.2 wt% $^{13}CH_3OH$ + 11.4 wt% glycerol aqueous solution	22.9	2.2	1.89

3.2.2. Quantification of methanol contribution to H_2 formation

Labeled $^{13}CH_3OH$ with $^{13}CO_2$ as a tracer was used to quantify the contribution of methanol and glycerol to the total hydrogen formation. These experiments were carried out over the best performing CZA-2-oxalate catalyst. First, two experiments with aqueous $^{12}CH_3OH$ and $^{13}CH_3OH$ at the standard reaction conditions were performed in order to provide the basis for the runs using the combined feedstock (Table 5). The first observation obtained from the methanol APR experiments was that the reaction rates were similar with the unlabeled and labeled feedstocks. The latter was not surprising as it is known that by replacing carbon-12 with carbon-13, the mass increases by only 8% thus not appreciably affecting the rate. The same catalytic behavior was observed for the combined reaction cycle (aqueous methanol-glycerol mixture, entries 3 and 4).

The quantitative contribution of methanol reforming to hydrogen formation was based on the CO_2 formation as CO_2 is a final product not undergoing further reactions and is by far the main C-containing product (selectivity over 98%) formed from methanol reforming. Based on the above, the contribution of methanol (with labeled ^{13}C) reforming to the formation of carbon dioxide in a test with glycerol can be quantified based on the ratio of *m/z*: 44/45 ($^{12}CO_2/^{13}CO_2$). From the results of the experiment number 4 it is concluded that for every 1 mol of $^{13}CO_2$ (formed from $^{13}CH_3OH$ reforming-reaction 1) 1.89 mol of $^{12}CO_2$ (formed from glycerol reforming-reaction (4)) are also produced. From the stoichiometry of the reforming reactions (1) and (4) it is calculated that methanol aqueous phase reforming contributes with 63% to the total CO_2 formed, while the remaining 37% results from glycerol reforming. Using the stoichiometry of the reforming reactions for the ratio H_2/CO_2, it is calculated that 68.7% of the total hydrogen formed originates from methanol reforming, while the rest derives from glycerol reforming. Going one step further, it is possible to calculate the percentage of glycerol that is converted via reforming to H_2 and CO_2. It was found that only 1.2% of the total glycerol reacted was consumed in the reforming pathway. Although methanol conversion

decreases when glycerol is present in the feedstock, the hydrogen formed is readily consumed from glycerol resulting in high glycerol conversion. These results confirm the ability of this type of catalytic materials (Cu:Zn:Al) to promote methanol reforming as well as glycerol hydrodeoxygenation tandem reaction cycle without consuming appreciable part of glycerol for the H_2 formation.

4. Conclusions

A novel one-pot catalytic route for the efficient conversion of bio-glycerol streams to propylene glycol has been developed and proposed for the first time. The formation of 1,2-propanediol using glycerol by-product as a raw material without the need of H_2 gas addition was realized. The present method takes advantage of the unreacted methanol that remains in the glycerol phase after transesterification and utilizes this methanol to produce the required H_2. Pt-supported and Cu bulk catalysts proved to be effective materials for the tandem reaction sequence (aqueous phase reforming and hydrogenolysis) producing selectively 1,2-propanediol under initial N_2 pressure. The Cu bulk catalysts of Cu:Zn:Al type and especially those prepared via the oxalate gel co-precipitation route showed superior performance with maximum 1,2-propanediol yield equal to 45% at low reaction temperatures (220 °C). Reaction rates of glycerol and methanol nicely correlate with the active surface of Cu area pointing to the decisive role of metallic Cu to methanol reforming and glycerol hydrodeoxygenation. The presence of residual Na in one of the catalytic samples prepared via the co-precipitation method is possibly the reason for the higher rates despite of the lower Cu area. The experiments using $^{12}CH_3OH$ and labeled $^{13}CH_3OH$ provided information about the source of the H_2 formed *in-situ*. It was shown that methanol reformation with water mainly contributed to hydrogen production, while the extent of glycerol aqueous phase reforming is limited. The encouraging experimental results obtained with the present catalyst provide the basis for further development of the novel catalytic process system for 1,2-propanediol production. Future work will be directed towards 1,2-propanediol yield improvement and catalyst stability study.

Acknowledgments

The project “Novel integrated process for the hydrogenolysis of bio-glycerol to 1,2-propanediol without hydrogen addition” is implemented under the “ARISTEIA” Action of the OPERATIONAL-PROGRAMME “EDUCATION AND LIFELONG LEARNING” Grant number 37 and is co-funded by the European Social Fund (ESF) and National Resources. Prof. Dion Vlachos, UDEL, USA is also acknowledged for providing the data on the binding energies for methanol and glycerol on Cu(1 1 1).

Appendix A. Supplementary data

Supplementary data associated with this article can be found, in the online version, at http://dx.doi.org/10.1016/j.apcatb.2014.08.004.

References

[1] M. Besson, P. Gallezot, C. Pinel, Chem. Rev. 114 (2014) 1827–1870.
[2] C.H. Zhou, H. Zhao, D.Sh. Tong, L.M. Wu, W.H. Yu, Catal. Rev. Sci. Eng. 55 (2013) 369–453.
[3] J. ten Damand, U. Hanefeld, ChemSusChem 4 (2011) 1017–1034.
[4] B. Katryniok, S. Paul, Fr. Dumeignil, ACS Catal. 3 (2013) 1819–1834.
[5] C.A. Henao, D. Simonetti, J.A. Dumesic, Ch.T. Maravelias, Comput. Aided Chem. Eng. 27 (2009) 1719–1724.
[6] J. Chaminand, L.A. Djakovitch, P. Gallezot, P. Marion, C. Pinel, C. Rosier, Green Chem. 6 (2004) 359–361.
[7] R.B. Mane, Ch.V. Rode, Green Chem. 14 (2012) 2780–2789.
[8] E.S. Vasiliadou, E. Heracleous, I.A. Vasalos, A.A. Lemonidou, Appl. Catal. B: Env. 92 (2009) 90–99.
[9] E.S. Vasiliadou, A.A. Lemonidou, Org. Process Res. Dev. 15 (2011) 925–931.
[10] J. Feng, J. Wang, Y. Zhou, H. Fu, H. Chen, X. Li, Chem. Lett. 36 (2007) 1274–1275.
[11] Z. Yuan, P. Wu, J. Gao, X. Lu, Z. Hou, X. Zheng, Catal. Lett. 130 (2009) 261–265.
[12] I. Gandarias, P.L. Arias, J. Requies, M.B. Guemez, J.L.G. Fierro, Appl. Catal. B: Env. 97 (2010) 248–256.
[13] J. Zhao, W. Yu, C. Chen, H. Miao, H. Ma, J. Xu, Catal. Lett. 134 (2010) 184–189.
[14] W. Yu, J. Xu, H. Ma, C. Chen, J. Zhao, H. Miao, Q. Song, Catal. Commun. 11 (2010) 493–497.
[15] E.S. Vasiliadou, A.A. Lemonidou, Appl. Catal. A: Gen. 396 (2011) 177–185.
[16] A. Bienholz, H. Hofmann, P. Claus, Appl. Catal. A: Gen. 391 (2011) 153–157.
[17] M.A. Dasari, P.P. Kiatsimkul, W.R. Sutterlin, G.J. Suppes, Appl. Catal. A: Gen. 281 (2005) 225–231.
[18] T. Jiang, Y. Zhou, Sh. Liang, H. Liu, B. Han, Green Chem. 11 (2009) 1000–1006.
[19] E. D'Hondt, St. Van de Vyver, B.F. Sels, P.A. Jacobs, Chem. Commun. 45 (2008) 6011–6012.
[20] A. Wawrzetz, B. Peng, A. Hrabar, A. Jentys, A.A. Lemonidou, J.A. Lercher, J. Catal. 269 (2009) 411–420.
[21] E. D'Hont, P. Jacobs, B. Sels, WO/2008/077205 (2008).
[22] D. Roy, B. Subramaniam, V.R. Chaudhari, Catal. Today 156 (2010) 31–37.
[23] A-Y. Yin, X-Y. Guo, W-L. Dai, K-N. Fan, Green Chem. 11 (2009) 1514–1516.
[24] R. Mane, Ch.V. Rode, Green Chem. 14 (2012) 2780–2789.
[25] M.L. Barbelli, G.F. Santori, N.N. Nichio, Bioresour. Technol. 111 (2012) 500–503.
[26] M.G. Musolino, L.A. Scarpino, Fr. Mauriello, R. Pietropaolo, Green Chem. 11 (2009) 1511–1513.
[27] I. Gandarias, P.L. Arias, J. Requies, M. El Doukkali, M.B. Güemez, J. Catal. 282 (2011) 237–247.
[28] I. Gandarias, P.L. Arias, S.G. Fernández, J. Requies, M. El Doukkali, M.B. Güemez, Catal. Today 195 (2012) 22–31.
[29] I. Gandarias, J. Requies, P.L. Arias, U. Armbruster, A. Martin, J. Catal. 290 (2012) 79–89.
[30] E.S. Vasiliadou, A.A. Lemonidou, Chem. Eng. J. 231 (2013) 103–112.
[31] A.A. Lemonidou, E. Vasileiadou, European Patent Office application, Application No EP11179515.9 (2011).
[32] G. Ertl, H. Knozinger, J. Weitkamp, Handbook of Heterogeneous Catalysis, vol. 2, Wiley-VCH, Germany, 1997.
[33] F. Chang, W. Kuo, K. Lee, Appl. Catal. A: Gen. 246 (2003) 253–264.
[34] S.D. Jones, L.M. Neal, H.E. Hagelin-Weaver, Appl. Catal. B: Env. 84 (2008) 631–642.
[35] X.-R. Zhang, L.-C. Wang, Ch.-Zh. Yao, Y. Cao, W.-L. Dai, H.-Y. He, K.-N. Fan, Catal. Lett. 102 (2005) 183–190.
[36] Zh. Huang, F. Cui, H. Kang, J. Chen, Ch. Xia, Appl. Catal. A: Gen. 366 (2009) 288–298.
[37] K.-W. Jun, W.-J. Shen1, K.S. Rama Rao, K.-W. Lee, Appl. Catal. A: Gen. 174 (1998) 231–238.
[38] R.R. Davda, J.W. Shabaker, G.W. Huber, R.D. Cortright, J.A. Dumesic, Appl. Catal. B Env. 56 (2005) 171–186.
[39] M. Balaraju, V. Rekha, P.S. Sai Prasad, R.B.N. Prasad, N. Lingaiah, Catal. Lett. 126 (2008) 119–124.
[40] T. Miyazawa, Y. Kusunoki, K. Kunimori, K. Tomishige, J. Catal. 240 (2006) 213–221.
[41] Y. Shinmi, S. Koso, T. Kubota, Y. Nakagawa, K. Tomishige, Appl. Catal. B. Env. 94 (2010) 318–326.
[42] T.L. Reitz, P.L. Lee, K.F. Czaplewski, J.C. Lang, K.E. Popp, H.H. Kung, J. Catal. 199 (2001) 193–201.
[43] M. Mrad, C. Gennequin, A. Aboukais, E. Abi-Aad, Catal. Today 176 (2011) 88–92.
[44] H. Oguchi, H. Kanai, K. Utani, Y. Matsumuraand, S. Imamura, Appl. Catal. A Gen. 293 (2005) 64–70.
[45] M. Turco, G. Bagnasco, C. Cammarano, P. Senese, U. Costantino, M. Sisani, Appl. Catal. B: Env. 77 (2007) 46–57.
[46] M. Kurtz, N. Bauer, Ch. Buscher, H. Wilmer, O. Hinrichsen, R. Becker, S. Rabe, K. Merz, M. Driess, R.A. Fischer, M. Muhler, Catal. Lett. 92 (2004) 49–52.
[47] A. Mastalir, B. Frank, H. Soerijanto, A. Deshpande, M. Niederberger, R. Schomacker, R. Schlogl, T. Ressler, J. Catal. 230 (2005) 464–475.
[48] Y. Chen, M. Salciccioli, D.G. Vlachos, J. Phys. Chem. C 115 (2011) 18707–18720.